Published in final edited form as:
Cell. 2007 March 9; 128(5): 901–913.

Mechanism of Actin Network Attachment to Moving Membranes:

Barbed End Capture by N-WASP WH2 Domains

Carl Co[1,2], **Derek T. Wong**[3], **Sarah Gierke**[1], **Vicky Chang**[1], and **Jack Taunton**[1,2]

1*Department of Cellular and Molecular Pharmacology, UCSF/UCB Cell Propulsion Lab (www.qb3.org/CPL), University of California, San Francisco, San Francisco, California 94158*

2*Program in Biological Sciences, UCSF/UCB Cell Propulsion Lab (www.qb3.org/CPL), University of California, San Francisco, San Francisco, California 94158*

3*Joint Graduate Group in Bioengineering, University of California, Berkeley and University of California, San Francisco Berkeley, California, 94720*

Summary

Actin filament networks exert protrusive and attachment forces on membranes and thereby drive membrane deformation and movement. Here, we show that N-WASP WH2 domains play a previously unanticipated role in vesicle movement by transiently attaching actin filament barbed ends to the membrane. To dissect the attachment mechanism, we reconstituted the propulsive motility of lipid-coated glass beads using purified soluble proteins. N-WASP WH2 mutants assembled actin comet tails and initiated movement, but the comet tails catastrophically detached from the membrane. When presented on the surface of a lipid-coated bead, WH2 domains were sufficient to maintain comet tail attachment. In v-Src-transformed fibroblasts, N-WASP WH2 mutants were severely defective in the formation of circular podosome arrays. In addition to creating an attachment force, interactions between WH2 domains and barbed ends may locally amplify signals for dendritic actin nucleation.

Introduction

Nucleation of branched actin filament networks occurs on the cytoplasmic surface of membranes. Actin polymerization generates force, which drives protrusion of the plasma membrane during cell motility (Pollard and Borisy, 2003), constriction and internalization of the plasma membrane during endocytosis (Kaksonen et al., 2003;Merrifield et al., 2005;Yarar et al., 2005), and the rocketing movement of endosomes and Golgi-derived vesicles (Kaksonen et al., 2000;Rozelle et al., 2000;Taunton et al., 2000). These processes are spatially and temporally coordinated by membrane-associated signaling complexes, often containing Rho-family GTPases (e.g., Cdc42 and Rac), phosphoinositides, and members of the WASP/WAVE/SCAR family of nucleation promoting factors.

Once activated at the membrane, WASP/WAVE/SCAR proteins directly activate the Arp2/3 complex via their conserved central/acidic (CA) domain, while the Arp2/3 complex binds simultaneously to the side of a membrane-proximal actin filament (Welch and Mullins, 2002). Delivery of an actin monomer to this pre-nucleation complex is mediated by the WASP Homology 2 domain (also called WH2, W, verprolin homology, or V domain), which is

correspondence: Jack Taunton, tel: (415) 514-2004, email: taunton@cmp.ucsf.edu

adjacent to the CA domain and is essential for actin nucleation by WASP/WAVE/SCAR proteins (Hufner et al., 2001;Marchand et al., 2001;Rohatgi et al., 1999). This event generates a new actin filament, with its fast-growing "barbed" end oriented toward the membrane and its "pointed" end anchored to the Arp2/3 complex at the new branch junction. WASP/WAVE/SCAR proteins dissociate from the Arp2/3 complex during branch formation (Egile et al., 2005;Martin et al., 2006;Uruno et al., 2003) and presumably remain bound to their activators at the membrane (e.g., Cdc42 or Rac and phosphoinositides). As inferred from electron micrographs of detergent-extracted lamellipodia (Bailly et al., 1999; Svitkina and Borisy, 1999), actin nucleation by the Arp2/3 complex generates a dense array of free barbed ends that are intimately associated with the advancing plasma membrane.

Our current understanding of how a dendritic actin network interacts with a surface derives primarily from in vitro reconstitution experiments (Upadhyaya et al., 2003;van der Gucht et al., 2005). Polystyrene beads containing immobilized Arp2/3 activators (ActA from Listeria monocytogenes, or the mammalian activators, WASP or N-WASP) assemble a dense "comet tail" of cross-linked actin filaments and undergo propulsive movement in cytoplasmic extracts (Cameron et al., 1999;Yarar et al., 1999) or in a mixture of purified proteins (Bernheim-Groswasser et al., 2002;Loisel et al., 1999;Wiesner et al., 2003). Similar to Listeria comet tails in extracts (Gerbal et al., 2000;Olbris and Herzfeld, 2000) and mammalian cells (Kuo and McGrath, 2000), comet tails assembled on polystyrene beads remain tightly attached to the bead surface (Cameron et al., 2001;Marcy et al., 2004). In addition, studies of ActA-coated liposomes and WASP WCA-coated oil droplets rocketing in cytoplasmic extracts indicate that actin comet tails exert attachment and compressive forces that distort these fluid surfaces (Boukellal et al., 2004;Giardini et al., 2003;Upadhyaya et al., 2003).

How a dendritic actin network exerts both attachment and compressive forces on a fluid membrane bilayer is a central, unresolved question in the field of actin-based motility. Here, we describe a novel biochemical reconstitution system to address this question in the context of vesicle movement powered by the Arp2/3 complex and N-WASP. Our results support a barbed end capture mechanism that explains how a dendritic actin network can remain persistently attached to a membrane while simultaneously pushing it forward. N-WASP WH2 domains mediate attachment by capturing barbed ends at the membrane surface, thereby permitting filament elongation while transiently protecting barbed ends from capping protein. N-WASP WH2 mutants that are defective in barbed end capture (but not Arp2/3 complex activation) are impaired in their ability to assemble large podosome arrays in v-Src-transformed fibroblasts. WH2 domains thus have multiple functions at the membrane in addition to their well-established role in promoting actin nucleation by the Arp2/3 complex.

Results

N-WASP WH2 domains localize to the attachment zone of moving vesicles

We initially considered two potential attachment mechanisms. In the first mechanism, attachment is mediated by the Arp2/3 complex, which transiently links the sides of membrane-proximal filaments to the CA domain of N-WASP prior to generating a new barbed end. This mechanism, for which there is little direct evidence, has been proposed to mediate attachment of actin comet tails to Listeria and ActA-coated particles (Giardini et al., 2003;Mogilner and Oster, 2003;Samarin et al., 2003). In the second mechanism, attachment is mediated by direct interactions between N-WASP and membrane-proximal barbed ends. This mechanism, for which there is also little evidence, is central to filament end-tracking models of Listeria movement (Dickinson et al., 2004;Dickinson and Purich, 2002). However, barbed end attachment to N-WASP need not be processive or coupled to ATP hydrolysis, as proposed in these models. As a third possibility, both side-binding and barbed end-binding mechanisms are required for attachment. We designed experiments to distinguish among these possibilities.

Previous immunofluorescence and immunoelectron microscopy studies indicated that N-WASP localizes asymmetrically on the surface of rocketing vesicles, at the interface between the actin network and the membrane (Taunton et al., 2000). One explanation for N-WASP asymmetry on a fluid membrane bilayer is that N-WASP directly interacts with a component of the actin comet tails (e.g., actin itself, the Arp2/3 complex, or another structural protein), as proposed for ActA-coated liposomes and WASP WCA-coated oil droplets (Boukellal et al., 2004;Giardini et al., 2003;Upadhyaya et al., 2003). In principle, these interactions could mediate attachment of the actin network to the membrane.

Based on this hypothesis, we searched for a candidate "attachment domain", operationally defined as the minimal N-WASP fragment that localizes to the membrane-actin interface of rocketing vesicles. We labeled a panel of bacterially expressed N-WASP fragments with fluorophores (Fig. 1A) and added them to phorbol ester-stimulated Xenopus egg extracts, a well-established system for studying vesicle motility (Ho et al., 2004;Papayannopoulos et al., 2005;Taunton et al., 2000). At the low concentrations used (50 nM), labeled N-WASP fragments had neither inhibitory nor stimulatory effects on vesicle motility, which is driven in these experiments by unlabeled endogenous N-WASP. We used live imaging to determine whether labeled fragments localized to the membrane-actin interface of moving vesicles, referred to here as the "attachment zone".

Deletion of the N-terminal region of N-WASP, which facilitated expression in E. coli, had no effect on asymmetric localization, as Alexa488-labeled N-WASP$^{151\text{-}501}$ localized to the attachment zone of every moving vesicle that we observed (Fig. 1B). In this experiment, we simultaneously imaged a rhodamine-labeled fragment comprising the polybasic and GTPase binding domains (rhod-BG). In contrast to N-WASP$^{151\text{-}501}$, rhod-BG was symmetrically distributed around the surface of every vesicle examined (Fig. 1B). Thus, interactions with acidic phospholipids and Cdc42, thought to be essential for the recruitment of N-WASP to endosomal vesicles in the Xenopus extract system (Ho et al., 2004;Papayannopoulos et al., 2005; Taunton, 2001), are not sufficient to mediate localization of BG to the attachment zone. We obtained identical results when we swapped fluorophores and imaged rhod-N-WASP$^{151\text{-}501}$ and Alexa488-BG, either separately or together (data not shown).

When the C-terminal WH2/central/acidic domains of N-WASP were fused to BG, the resulting BG-WCA fragment now localized to the attachment zone (Fig. 1C), suggesting that an attachment domain lies within the Arp2/3 complex-activating region of N-WASP. Given that the Arp2/3 complex can simultaneously bind WCA and the side of an actin filament (Marchand et al., 2001), it seemed like an excellent candidate for mediating attachment, as proposed for Listeria motility (Giardini et al., 2003;Mogilner and Oster, 2003;Samarin et al., 2003). We were therefore surprised that BG-W, which lacks the Arp2/3-binding central and acidic domains, strongly localized to the attachment zone (Fig. 1C). A minimal fragment comprising only the polybasic and WH2 domains (B-W) also localized to the attachment zone (Fig. 1C). In time-lapse sequences, B-W precisely colocalized with the membrane/actin interface during vesicle movement (Movie 1), whereas the isolated polybasic, WH2, and WCA fragments did not localize to vesicles at all (data not shown). The asymmetric localization of all WH2 domain-containing fragments suggested a novel function for this domain, independent of its essential role in promoting actin nucleation by the Arp2/3 complex.

We searched for point mutations in the N-WASP WH2 domains that would selectively abrogate the putative attachment function without affecting Arp2/3-promoted actin nucleation. Because N-WASP has two partially redundant WH2 domains (Yamaguchi et al., 2000), we deleted one of them, providing a construct hereafter referred to as "WT N-WASP" (Fig. 2A). We characterized two WH2 domain mutants, K444Q and R438A. Relative to WT N-WASP (K_d=0.9 μM), K444Q binds actin monomers with ~10-fold lower affinity (K_d=10 μM), and

R438A binds with at least 30-fold lower affinity ($K_d \geq 30$ μM), based on fluorescence anisotropy assays (Marchand et al., 2001) (Fig. 2B). Despite the significant decrease in actin binding affinity, both WH2 mutants had nucleation promoting activity comparable to WT N-WASP (Fig. 2C and S1). Thus, high-affinity actin binding by the WH2 domain is not required for potent nucleation promoting activity, as noted in previous studies of WASP WH2 mutants (Marchand et al., 2001).

Strikingly, neither R438A nor K444Q N-WASP (labeled with Alexa488) localized to the attachment zone of rocketing vesicles when added to Xenopus egg extracts (Fig. 2D). By contrast, Alexa594-labeled WT N-WASP, imaged on the same moving vesicles, localized exclusively to the attachment zone. These results are remarkable: single mutations in the WH2 domain, both of which reduce actin binding affinity, abolish asymmetric localization to the actin/membrane interface without affecting nucleation promoting activity.

Reconstitution of membrane movement from pure components: WH2 mutations induce catastrophic detachment of actin comet tails

To dissect the mechanism of actin/membrane attachment, we compared WT, R438A, and K444Q N-WASP in a novel reconstitution system using purified components (Fig. 3A). Our system is similar to one used previously to study N-WASP-dependent motility of polystyrene beads and Listeria (Bernheim-Groswasser et al., 2002;Loisel et al., 1999), with two important differences. First, our motility substrate consists of a lipid bilayer (5:75:20, PIP2:PC:PS) supported on the surface of 2.3 μm glass beads. Second, to activate N-WASP, we reconstituted a Cdc42 signaling pathway that includes intersectin, a Cdc42-specific guanine nucleotide exchange factor (Hussain et al., 2001), and prenylated Cdc42 bound to its endogenous inhibitor, RhoGDI (Hoffman et al., 2000). In the presence of GTPγS and the soluble Cdc42/RhoGDI complex, a constitutively active intersectin fragment promoted the translocation of N-WASP to the surface of lipid-coated beads (Fig. S2).

Following Cdc42/N-WASP activation, lipid-coated beads were added to a motility mix containing actin, the Arp2/3 complex, capping protein, and profilin. Cofilin was omitted to prevent disassembly of the actin comet tails. Actin comet tails formed on 100% of the beads within 5 minutes, resulting in propulsive motility at 0.58 ± 0.20 μm/min (Movie 2), similar to previously published speeds with N-WASP-coated polystyrene beads (Wiesner et al., 2003). At early time points (5 min after mixing components), there were no major differences between motility reactions containing WT, R438A, or K444Q N-WASP (Fig. 3B). The average speed of the WH2 mutants was slightly faster (R438A, 0.85±0.26 μm/min, $p<0.005$, T-test) or similar (K444Q, 0.64±0.12 μm/min) compared to WT N-WASP (Fig. S3).

Within 10-30 min, lipid-coated beads containing R438A or K444Q N-WASP spontaneously detached from their comet tails, whereas nearly all of the beads containing WT N-WASP remained attached to their tails (Fig. 3B,D). Time-lapse movies revealed sudden, catastrophic separation of the lipid-coated beads from their intact tails; after detaching, the beads moved randomly under the influence of Brownian forces and bulk liquid flow (Fig. 3C and Movie 3). Quantification of fixed motility reactions demonstrated progressive comet tail detachment over time, with R438A-assembled comet tails detaching more rapidly than K444Q-assembled tails (Fig. 3D). Addition of a fresh supply of actin monomers to motility reactions in which 100% of the lipid-coated beads had lost their tails resulted in comet tail re-formation and movement of 100% of the beads, and increasing the initial actin concentration from 6 μM to 9 μM delayed comet tail detachment in motility reactions containing R438A and K444Q N-WASP (Fig. S4). Thus, time-dependent comet tail detachment most likely results from the gradual depletion of actin monomers from solution.

Our results suggest that actin binding by the WH2 domain plays a critical role in the attachment mechanism, but they do not rule out an additional requirement for N-WASP binding to the Arp2/3 complex. To test this possibility directly, we treated motility reactions with the N-WASP CA fragment (fused to GST), a potent competitive inhibitor of the Arp2/3 complex (Hufner et al., 2001;Rohatgi et al., 1999). GST-CA rapidly arrested comet tail growth and bead movement, but it had no effect on comet tail attachment (Fig. S5). This result argues against a requirement for N-WASP-Arp2/3 interactions in the attachment mechanism.

Barbed end capture by WH2 domains is necessary and sufficient to maintain comet tail attachment

WH2 domains bind in a small cleft at the barbed end of an actin monomer (Chereau et al., 2005;Hertzog et al., 2004) and are thought to transiently interact with filament barbed ends while promoting elongation (Egile et al., 1999;Higgs et al., 1999). Superposition of the WASP WH2/actin structure and the Holmes filament model suggested that the barbed end of a filament could accommodate a WH2 domain without any steric clashes (Chereau et al., 2005). These biochemical and structural properties, together with the inverse correlation between actin binding affinity (WT>K444Q>R438A, Fig. 2B) and the rate of comet tail detachment (R438A>K444Q>WT, Fig. 3D), led us to hypothesize that WH2-mediated capture of membrane-proximal barbed ends plays a critical role in the attachment mechanism. Barbed end capture could be direct or it could involve WH2-mediated delivery of ATP-actin monomers.

To test the dependence of comet tail attachment on actin barbed ends, we acutely perturbed motility reactions after assembling comet tails for 10 min. Four-fold dilution of motility reactions containing WT N-WASP induced comet tail detachment from ~50% of the lipid-coated beads after 15 min, an effect that was largely suppressed by including actin monomers (1 μM) in the dilution buffer (Fig. 4A). By contrast, dilution of motility reactions into actin plus increasing concentrations of capping protein induced catastrophic tail detachment, with 100% detachment occurring at 500 nM capping protein. The actin monomer sequestering drug, latrunculin, delayed but did not prevent comet tail detachment induced by excess capping protein (Fig. S6). This dramatic stabilizing effect may be explained, in part, by latrunculin's ability to prevent the depletion of ATP-actin, which may be required to link filament barbed ends to membrane-bound WH2 domains.

We sought direct evidence for the formation of a complex between N-WASP and actin filament barbed ends in the absence of the Arp2/3 complex. We adapted an imaging-based filament capture assay (Bear et al., 2002;Samarin et al., 2003) using N-WASP-coated polystyrene beads and Alexa488 phalloidin-stabilized actin filaments. We quantified Alexa488 fluorescence on the surface of individual beads as a function of increasing amounts of rhodamine-labeled, latrunculin-stabilized actin monomers. Whereas Alexa488 filaments alone did not stably associate with the N-WASP-coated beads, filaments were robustly captured in the presence of rhod-actin monomers (Fig. 4B,C). Binding of Alexa488 filaments to N-WASP-coated beads was prevented by capping protein, confirming barbed end association. The inability of immobilized N-WASP to directly capture phalloidin-stabilized filaments (containing primarily ADP and ADP-P_i) may be due to a requirement for ATP-actin, supplied here in the form of nonpolymerizable latrunculin/actin/ATP complexes. The ability of a WH2/latrunculin/actin complex to productively interact with a barbed end-like structure has been observed previously in the context of WCA activation of Arp2/3, a functional and possibly structural analog of a barbed end (Dayel and Mullins, 2004).

Filament capture was abrogated by the R438A and K444Q mutations in a manner that correlated with their actin monomer binding affinities (Fig. 4C). Quantification of bead-associated rhodamine fluorescence as a function of latrunculin/actin provided actin binding

curves for WT, R438A, and K444Q N-WASP (Fig. S7) that were qualitatively similar to those obtained in the bulk solution anisotropy assay (Fig. 2B). We also compared the Cdc42-binding BG fragment with the WH2-containing BG-W fragment; only the BG-W fragment captured actin filaments (Fig. S8). Together, these results indicate that a high surface density of WH2 domains, bound to actin monomers, can capture actin filament barbed ends in the absence of other proteins.

We next tested whether barbed end capture by N-WASP WH2 domains is sufficient to mediate attachment of a dendritic actin network to a fluid membrane bilayer. We took advantage of the fact that N-WASP dynamically exchanges between the membrane and solution to ask whether replacement of membrane-bound N-WASP with BG or BG-W fragments could maintain comet tail attachment (Fig. 5A). Actin comet tails were first assembled for 12 min on lipid-coated beads containing activated Cdc42 and Alexa488 N-WASP (5% labeled, final concentration of 150 nM). Addition of either BG or BG-W (2 μM) resulted in the displacement of Alexa488 N-WASP from the beads ($t_{1/2}$∼5 minutes, Fig. 5B), whereas N-WASP fluorescence increased slightly in control reactions to which buffer was added. As expected, replacement of N-WASP by BG caused 100% of the comet tails to detach with a time course that paralleled N-WASP dissociation (Fig. 5B,C and Movie 4). Remarkably, most of the actin comet tails remained attached to the lipid-coated beads for at least 45 min after addition of BG-W, indicating that WH2 domains are sufficient to mediate comet tail attachment. Comet tail growth was abolished by BG-W (Fig. 5D), consistent with a requirement for Arp2/3-promoted nucleation and branching to sustain forward movement.

WH2 mutations disrupt podosome organization in v-Src-transformed cells

N-WASP promotes the assembly of protrusive actin-based structures called podosomes (or invadopodia) in v-Src-transformed fibroblasts (Mizutani et al., 2002) and breast carcinoma cells (Yamaguchi et al., 2005). To test whether WH2-mediated actin attachment plays a role in podosome assembly and organization, we transduced v-Src^{+}/N-$WASP^{-/-}$ fibroblasts with retroviruses encoding full-length GFP-N-WASP or an N-WASP mutant in which the conserved arginine in each WH2 domain was mutated to alanine (R410A/R438A, “RA/RA”). Consistent with our earlier results (Fig. 2C), the RA/RA mutant was essentially identical to wild-type N-WASP in pyrene actin nucleation assays (Fig. S9). After retroviral transduction and FACS-sorting, we obtained WT and RA/RA GFP-N-WASP cells that expressed similar levels of GFP-N-WASP and v-Src (Fig. 6A). The cells also expressed similar levels of VASP, which has a WH2-related domain and has been localized to podosomes/invadopodia (Dutartre et al., 1996;Spinardi et al., 2004).

Consistent with previous dominant negative and siRNA experiments (Mizutani et al., 2002; Yamaguchi et al., 2005), v-Src^{+}/N-$WASP^{-/-}$ cells were devoid of podosomes, whether left untreated or transduced with a GFP retrovirus (data not shown). By contrast, we observed podosomes in both the WT (50±6%) and RA/RA cells (38±7%, mean±S.D., three independent experiments). To test for differences in podosome size and organization, we focused on the podosome-containing cells from three independent datasets (quantification was performed blind). We quantified the percentage of these cells that contained “bars” (length/width ≥3; see Fig. 6B(ii), for example) and “rings” (contiguous circular arrays of podosomes; see Fig. 6B(i), for example). Compared to the RA/RA cells, twice as many WT cells had podosome bars or rings (Fig. 6C, $p<0.03$, T-test). Moreover, WT cells were ∼10 times more likely than RA/RA cells to assemble rings (Fig. 6D, $p<0.01$). We obtained similar results with a second batch of FACS-sorted cells that expressed higher levels of WT and RA/RA GFP-N-WASP (data not shown).

We measured the size (area) of individual bars, rings, and puncta, restricting our analysis to WT and RA/RA cells that had at least one podosome bar or ring. Large podosomes (>20

μm^2) were ~5 times more abundant in WT cells (Fig. 6E), although the average number of podosomes per cell was similar for WT and RA/RA cells. We conclude that RA/RA N-WASP is defective in the assembly of large podosome arrays in v-Src-transformed fibroblasts. These results suggest that N-WASP clustering, mediated by WH2/barbed end interactions, plays a role in the propagation and/or stabilization of extended podosome networks.

Discussion

The central finding of this study is that WH2 domains mediate the dynamic attachment of actin filament barbed ends to the membrane during N-WASP-driven membrane movement. Highly concentrated at the actin/membrane interface, N-WASP WH2 domains maintain a persistent connection between the dendritic network and the advancing membrane of a rocketing vesicle. The Arp2/3 complex or VASP, which protects barbed ends from capping protein via a WH2-like actin-binding domain (Barzik et al., 2005), may coordinate attachment and detachment of actin filaments to moving Listeria (Laurent et al., 1999;Samarin et al., 2003). VASP (Bear et al., 2002;Samarin et al., 2003), along with its recently identified partner, lamellipodin (Krause et al., 2004), are also likely to be important regulators of actin attachment at the leading edge of migrating cells. In the context of podosome assembly (Fig. 6), VASP and N-WASP clearly have nonredundant functions.

Multiple lines of biochemical evidence support our proposed barbed end attachment mechanism. First, WH2 domains are necessary and sufficient to localize N-WASP fragments to sites of dendritic actin nucleation on the surface of rocketing vesicles (Fig. 1). Second, R438A and K444Q WH2 mutations prevent localization to the attachment zone, yet have no effect on Arp2/3-dependent actin nucleation (Fig. 2). Third, in a reconstituted membrane motility system, WH2 domains are necessary (Fig. 3) and sufficient (Fig. 5) to maintain comet tail attachment to lipid-coated beads. Fourth, high concentrations of capping protein accelerate comet tail detachment (Fig, 4A and S6). Fifth, immobilized actin monomer/WH2 complexes capture actin filament barbed ends in the absence of other proteins (Fig. 4B).

Model for WH2-mediated attachment of actin filament barbed ends to the membrane

Our model for actin/membrane attachment extends the dendritic nucleation model (Mullins et al., 1998) by considering the fate of barbed ends at the membrane surface (Fig. 7A), which cycle through elongation, attachment, and release steps until filament growth and membrane attachment are ultimately terminated by capping protein. Reversible capture of a membrane-proximal barbed end by WH2 or WH2/actin establishes the molecular link between the dendritic network and the membrane. It is not clear whether barbed end capture occurs primarily via free WH2 domains or WH2/actin monomers. Based on the preference of WASP WH2 for ATP-actin (5-fold higher binding affinity relative to ADP-actin) (Chereau et al., 2005), it is possible that barbed end binding by free WH2 domains is sensitive to the nucleotide state of the terminal actin subunit. This effect may be exacerbated by the R438A and K444Q mutations, leading to catastrophic detachment of the actin network as the concentration of ATP-actin declines.

A barbed end attachment model may seem counterintuitive given the high dissociation rate of WH2 from barbed ends in solution (2500 s^{-1} if similar to the profilin-barbed end dissociation rate, Vavylonis et al., 2006). This dissociation rate has not been measured, but it must be fast because the rate of barbed end polymerization is only slightly affected by saturating concentrations of WH2-containing peptides (Egile et al., 1999;Higgs et al., 1999). Nevertheless, in the context of a dendritic actin network attached to a membrane surface, rebinding of a free barbed end to a WH2 domain or WH2/actin complex is likely to be rapid. First, the surface density (or “local concentration”) of N-WASP on moving lipid-coated beads is high, estimated from fluorescence measurements to be ~50,000 molecules per μm^2, with a

maximum distance between N-WASP molecules of ~5 nm (unpublished results). Second, actin filaments in the attachment zone are cross-linked in a dendritic network, and thus their movement is highly constrained. Ligand rebinding effects between membrane-associated N-WASP and membrane-proximal barbed ends most likely drive the attachment interaction, despite the low affinity of WH2 domains for filament barbed ends in solution.

Our model resembles filament end-tracking models for Listeria motility (Dickinson et al., 2004;Dickinson and Purich, 2002) in that barbed ends, rather than filament sides or nascent branches, mediate attachment to the membrane. A key difference, however, is that WH2 domains need not act as processive end-tracking proteins dependent on ATP hydrolysis by actin (although WH2/barbed end affinity may be modulated by ATP hydrolysis). Individual barbed ends can dissociate from the membrane because attachment is mediated by a multivalent array of hundreds or thousands of cross-linked filaments. Disruption of WH2/barbed end attachment interactions may be rate-limiting for vesicle movement, as suggested by recent experimental (Soo and Theriot, 2005) and computational (Alberts and Odell, 2004) studies of Listeria movement. The increased speed of lipid-coated beads driven by R438A N-WASP before they detach is consistent with this idea (Fig. S3).

Capture of diffusing N-WASP molecules by nascent barbed ends: a potential mechanism for signal amplification

In the context of a rocketing vesicle, WH2 domains are necessary and sufficient to localize N-WASP fragments to membrane sites enriched in nascent barbed ends (Fig. 1C and 2D). Although we have focused primarily on attachment of the actin network to moving vesicles, our results imply that barbed ends can reciprocally capture a pool of diffusing N-WASP molecules at membrane sites of dendritic actin nucleation. This suggests a mechanism for localized signal amplification, which is likely defective in WH2 mutants (Fig. 7B). Reversible capture of diffusing N-WASP molecules by nascent barbed ends increases the frequency of local nucleation and branching events, resulting in the expansion of the dendritic network. The reduced number of large podosome arrays assembled by RA/RA N-WASP (Fig. 6) is consistent with this proposal. Although the mechanism of podosome assembly is largely unknown, we speculate that N-WASP capture by nascent barbed ends is a critical determinant of podosome expansion, fusion and/or fragmentation. Similarly, WH2-mediated capture of WAVE/SCAR proteins by nascent barbed ends may locally amplify actin nucleation signals at the leading edge of moving cells.

Experimental Procedures

Protein expression, purification and fluorescent labeling

N-WASP fragments were amplified by PCR from full-length rat N-WASP and mini-N-WASP (BG-WCA) (Prehoda et al., 2000) and expressed as His_6-HA-tagged fusion proteins in E. coli (all constructs verified by DNA sequencing). After Ni-NTA purification, the His_6 tag was cleaved with TEV protease. Proteins were further purified by chromatography over HiTRAP S, Q, or heparin columns (Amersham).

Actin was purified from rabbit skeletal muscle (Pardee and Spudich, 1982) and labeled with pyrene iodoacetamide (Cooper et al., 1983), Alexa488-NHS, or rhodamine-NHS (Molecular Probes) (Isambert et al., 1995). Arp2/3 complex was purified from bovine brain (Egile et al., 1999). Capping protein was expressed in E. coli and purified as described (Palmgren et al., 2001). Cdc42/RhoGDI complex was expressed and purified as described (Hoffman et al., 2000). Intersectin DH-PH was expressed in E. coli (Zamanian and Kelly, 2003). Profilin (purified from A. castellanii) was a gift from Mark Dayel and Dyche Mullins (UCSF). GST-

CA (derived from human N-WASP and expressed in E. coli) was a gift from Bill Brieher and Tim Mitchison (Harvard Medical School).

For fluorescent labeling of N-WASP fragments, maleimide dyes (Molecular Probes) were added at a 20-fold molar excess and incubated for 2 h at RT or overnight at 4°C. Reactions were quenched with 5 mM β-mercaptoethanol for 15 min, and fluorescent proteins were purified over HiTRAP S, Q, or heparin columns. For fluorescence anisotropy assays, Oregon Green-labeled WCA proteins were purified by S200 gel filtration chromatography. Fluorescence anisotropy was measured using an ANALYST AD fluorescence plate reader. WT and mutant Oregon Green-labeled WCA (100 nM) were equilibrated with increasing concentrations of actin monomers, and anisotropy data were fit to a quadratic binding equation to determine the K_d.

Attachment zone localization assay

Vesicle motility reactions in Xenopus egg extracts were performed as described (Taunton et al., 2000). Fluorescence and phase contrast images were acquired for ~50 rocketing vesicles (Olympus I×70 microscope; Coolsnap HQ CCD camera). Image analysis was performed with ImageJ.

Reconstitution of membrane movement

Liposomes (5:75:25, PIP2:PC:PS) were fused to the surface of glass beads (Bangs laboratories, 2.3 μm diameter) to create a supported lipid bilayer. Lipid-coated beads were incubated with 1.5 μM Cdc42/RhoGDI complex, 2 μM DH-PH, and 100 μM GTPγS for 10 min at RT, followed by addition of 1.5 μM N-WASP for 10 min. Motility reactions were initiated by diluting the suspension of N-WASP/Cdc42/lipid-coated glass beads 10-fold into motility buffer (10 mM imidazole [pH 7.0], 50 mM KCl, 1 mM $MgSO_4$, 1 mM EGTA, 5 mg/ml BSA, 0.2% methylcellulose, 5 mM TCEP, 1 mM ATP, 7.5 mM creatine phosphate, 1.25 mM DABCO) containing the following proteins: 6 μM G-actin, 0.075 μM Arp2/3, 0.05 μM capping protein, 2 μM profilin. Additional details are provided in the Supplemental Data.

Actin filament capture assay

Polystyrene beads (2.0 μm, Polysciences) were coated with 1 μM N-WASP in F-buffer (10 mM imidazole pH 7, 0.05 M KCl, 1 mM $MgCl_2$, 1 mM EGTA) for 1 h, washed, and stored in 1 mg/ml BSA. Actin (8 μM) was polymerized in F-buffer for 2 h and stabilized with 6 μM Alexa488 phalloidin to give "Alexa488 filaments". N-WASP beads (5.73×10^8 beads/ml) were rotated with Alexa488 filaments (4 μM) in the presence of varying concentrations of rhod-actin monomers (stabilized with a 10-fold molar excess of latrunculin). After 10 min, the suspension was diluted 5-fold into F-buffer containing 1 mg/ml BSA. Randomly chosen beads (15-20) were imaged by phase contrast and fluorescence microscopy.

Podosome assay

v-Src-transformed N-WASP$^{-/-}$ mouse embryonic fibroblasts (made from the parental N-WASP$^{-/-}$ cells, Papayannopoulos et al., 2005;Snapper et al., 2001), were transduced with retroviruses encoding GFP-fused WT or R410A/R438A (RA/RA) N-WASP and FACS-sorted. Cells were plated on fibronectin-coated coverslips, and after 24 hours, fixed with 4% formaldehyde and stained with Alexa594-phalloidin. In each experiment, images were acquired from two coverslips (40X objective, 150 microscope fields per coverslip). Images were analyzed as described in the main text and figure legends. Researchers were blinded to the identity of the datasets during image analysis.

Supplementary Material

Refer to Web version on PubMed Central for supplementary material.

Acknowledgements

This work was supported by the NIH (GM066229). D.T.W. acknowledges support from the UCSF/UCB NIH Nanomedicine Development Center (PN2 EY016546). We thank Orkun Akin, Mark Dayel, and Dyche Mullins for helpful discussions regarding the reconstituted motility system. We are grateful to Orion Weiner and Daniel Fletcher for comments on the manuscript.

References

Alberts JB, Odell GM. In silico reconstitution of Listeria propulsion exhibits nano-saltation. PLoS Biol 2004;2:e412. [PubMed: 15562315]

Bailly M, Macaluso F, Cammer M, Chan A, Segall JE, Condeelis JS. Relationship between Arp2/3 complex and the barbed ends of actin filaments at the leading edge of carcinoma cells after epidermal growth factor stimulation. J Cell Biol 1999;145:331–345. [PubMed: 10209028]

Barzik M, Kotova TI, Higgs HN, Hazelwood L, Hanein D, Gertler FB, Schafer DA. Ena/VASP proteins enhance actin polymerization in the presence of barbed end capping proteins. J Biol Chem 2005;280:28653–28662. [PubMed: 15939738]

Bear JE, Svitkina TM, Krause M, Schafer DA, Loureiro JJ, Strasser GA, Maly IV, Chaga OY, Cooper JA, Borisy GG, Gertler FB. Antagonism between Ena/VASP proteins and actin filament capping regulates fibroblast motility. Cell 2002;109:509–521. [PubMed: 12086607]

Bernheim-Groswasser A, Wiesner S, Golsteyn RM, Carlier MF, Sykes C. The dynamics of actin-based motility depend on surface parameters. Nature 2002;417:308–311. [PubMed: 12015607]

Boukellal H, Campas O, Joanny JF, Prost J, Sykes C. Soft Listeria: actin-based propulsion of liquid drops. Phys Rev E Stat Nonlin Soft Matter Phys 2004;69:061906. [PubMed: 15244616]

Cameron LA, Footer MJ, van Oudenaarden A, Theriot JA. Motility of ActA protein-coated microspheres driven by actin polymerization. Proc Natl Acad Sci U S A 1999;96:4908–4913. [PubMed: 10220392]

Cameron LA, Svitkina TM, Vignjevic D, Theriot JA, Borisy GG. Dendritic organization of actin comet tails. Curr Biol 2001;11:130–135. [PubMed: 11231131]

Chereau D, Kerff F, Graceffa P, Grabarek Z, Langsetmo K, Dominguez R. Actin-bound structures of Wiskott-Aldrich syndrome protein (WASP)-homology domain 2 and the implications for filament assembly. Proc Natl Acad Sci U S A 2005;102:16644–16649. [PubMed: 16275905]

Cooper JA, Walker SB, Pollard TD. Pyrene actin: documentation of the validity of a sensitive assay for actin polymerization. J Muscle Res Cell Motil 1983;4:253–262. [PubMed: 6863518]

Dayel MJ, Mullins RD. Activation of Arp2/3 complex: addition of the first subunit of the new filament by a WASP protein triggers rapid ATP hydrolysis on Arp2. PLoS Biol 2004;2:E91. [PubMed: 15094799]

Dickinson RB, Caro L, Purich DL. Force generation by cytoskeletal filament end-tracking proteins. Biophys J 2004;87:2838–2854. [PubMed: 15454475]

Dickinson RB, Purich DL. Clamped-filament elongation model for actin-based motors. Biophys J 2002;82:605–617. [PubMed: 11806905]

Dutartre H, Davoust J, Gorvel JP, Chavrier P. Cytokinesis arrest and redistribution of actin-cytoskeleton regulatory components in cells expressing the Rho GTPase CDC42Hs. J Cell Sci 1996;109(Pt 2): 367–377. [PubMed: 8838660]

Egile C, Loisel TP, Laurent V, Li R, Pantaloni D, Sansonetti PJ, Carlier MF. Activation of the CDC42 effector N-WASP by the Shigella flexneri IcsA protein promotes actin nucleation by Arp2/3 complex and bacterial actin-based motility. J Cell Biol 1999;146:1319–1332. [PubMed: 10491394]

Egile C, Rouiller I, Xu XP, Volkmann N, Li R, Hanein D. Mechanism of filament nucleation and branch stability revealed by the structure of the Arp2/3 complex at actin branch junctions. PLoS Biol 2005;3:e383. [PubMed: 16262445]

Gerbal F, Laurent V, Ott A, Carlier MF, Chaikin P, Prost J. Measurement of the elasticity of the actin tail of Listeria monocytogenes. Eur Biophys J 2000;29:134–140. [PubMed: 10877022]

Giardini PA, Fletcher DA, Theriot JA. Compression forces generated by actin comet tails on lipid vesicles. Proc Natl Acad Sci U S A 2003;100:6493–6498. [PubMed: 12738883]

Hertzog M, van Heijenoort C, Didry D, Gaudier M, Coutant J, Gigant B, Didelot G, Preat T, Knossow M, Guittet E, Carlier MF. The beta-thymosin/WH2 domain; structural basis for the switch from inhibition to promotion of actin assembly. Cell 2004;117:611–623. [PubMed: 15163409]

Higgs HN, Blanchoin L, Pollard TD. Influence of the C terminus of Wiskott-Aldrich syndrome protein (WASp) and the Arp2/3 complex on actin polymerization. Biochemistry 1999;38:15212–15222. [PubMed: 10563804]

Ho HY, Rohatgi R, Lebensohn AM, Le M, Li J, Gygi SP, Kirschner MW. Toca-1 mediates Cdc42-dependent actin nucleation by activating the N-WASP-WIP complex. Cell 2004;118:203–216. [PubMed: 15260990]

Hoffman GR, Nassar N, Cerione RA. Structure of the Rho family GTP-binding protein Cdc42 in complex with the multifunctional regulator RhoGDI. Cell 2000;100:345–356. [PubMed: 10676816]

Hufner K, Higgs HN, Pollard TD, Jacobi C, Aepfelbacher M, Linder S. The verprolin-like central (vc) region of Wiskott-Aldrich syndrome protein induces Arp2/3 complex-dependent actin nucleation. J Biol Chem 2001;276:35761–35767. [PubMed: 11459849]

Hussain NK, Jenna S, Glogauer M, Quinn CC, Wasiak S, Guipponi M, Antonarakis SE, Kay BK, Stossel TP, Lamarche-Vane N, McPherson PS. Endocytic protein intersectin-l regulates actin assembly via Cdc42 and N-WASP. Nat Cell Biol 2001;3:927–932. [PubMed: 11584276]

Kaksonen M, Peng HB, Rauvala H. Association of cortactin with dynamic actin in lamellipodia and on endosomal vesicles. J Cell Sci 2000;113(Pt 24):4421–4426. [PubMed: 11082035]

Kaksonen M, Sun Y, Drubin DG. A pathway for association of receptors, adaptors, and actin during endocytic internalization. Cell 2003;115:475–487. [PubMed: 14622601]

Krause M, Leslie JD, Stewart M, Lafuente EM, Valderrama F, Jagannathan R, Strasser GA, Rubinson DA, Liu H, Way M, et al. Lamellipodin, an Ena/VASP ligand, is implicated in the regulation of lamellipodial dynamics. Dev Cell 2004;7:571–583. [PubMed: 15469845]

Laurent V, Loisel TP, Harbeck B, Wehman A, Grobe L, Jockusch BM, Wehland J, Gertler FB, Carlier MF. Role of proteins of the Ena/VASP family in actin-based motility of Listeria monocytogenes. J Cell Biol 1999;144:1245–1258. [PubMed: 10087267]

Loisel TP, Boujemaa R, Pantaloni D, Carlier MF. Reconstitution of actin-based motility of Listeria and Shigella using pure proteins. Nature 1999;401:613–616. [PubMed: 10524632]

Marchand JB, Kaiser DA, Pollard TD, Higgs HN. Interaction of WASP/Scar proteins with actin and vertebrate Arp2/3 complex. Nat Cell Biol 2001;3:76–82. [PubMed: 11146629]

Marcy Y, Prost J, Carlier MF, Sykes C. Forces generated during actin-based propulsion: a direct measurement by micromanipulation. Proc Natl Acad Sci U S A 2004;101:5992–5997. [PubMed: 15079054]

Martin AC, Welch MD, Drubin DG. Arp2/3 ATP hydrolysis-catalysed branch dissociation is critical for endocytic force generation. Nat Cell Biol 2006;8:826–833. [PubMed: 16862144]

Merrifield CJ, Perrais D, Zenisek D. Coupling between clathrin-coated-pit invagination, cortactin recruitment, and membrane scission observed in live cells. Cell 2005;121:593–606. [PubMed: 15907472]

Mogilner A, Oster G. Force generation by actin polymerization II: the elastic ratchet and tethered filaments. Biophys J 2003;84:1591–1605. [PubMed: 12609863]

Mullins RD, Heuser JA, Pollard TD. The interaction of Arp2/3 complex with actin: nucleation, high affinity pointed end capping, and formation of branching networks of filaments. Proc Natl Acad Sci U S A 1998;95:6181–6186. [PubMed: 9600938]

Olbris DJ, Herzfeld J. Reconstitution of Listeria motility: implications for the mechanism of force transduction. Biochim Biophys Acta 2000;1495:140–149. [PubMed: 10656971]

Palmgren S, Ojala PJ, Wear MA, Cooper JA, Lappalainen P. Interactions with PIP2, ADP-actin monomers, and capping protein regulate the activity and localization of yeast twinfilin. J Cell Biol 2001;155:251–260. [PubMed: 11604420]

Papayannopoulos V, Co C, Prehoda KE, Snapper S, Taunton J, Lim WA. A polybasic motif allows N-WASP to act as a sensor of PIP(2) density. Mol Cell 2005;17:181–191. [PubMed: 15664188]

Pardee JD, Spudich JA. Purification of muscle actin. Methods Cell Biol 1982;24:271–289. [PubMed: 7098993]

Pollard TD, Borisy GG. Cellular motility driven by assembly and disassembly of actin filaments. Cell 2003;112:453–465. [PubMed: 12600310]

Prehoda KE, Scott JA, Mullins RD, Lim WA. Integration of multiple signals through cooperative regulation of the N-WASP-Arp2/3 complex. Science 2000;290:801–806. [PubMed: 11052943]

Rohatgi R, Ma L, Miki H, Lopez M, Kirchhausen T, Takenawa T, Kirschner MW. The interaction between N-WASP and the Arp2/3 complex links Cdc42-dependent signals to actin assembly. Cell 1999;97:221–231. [PubMed: 10219243]

Rozelle AL, Machesky LM, Yamamoto M, Driessens MH, Insall RH, Roth MG, Luby-Phelps K, Marriott G, Hall A, Yin HL. Phosphatidylinositol 4,5-bisphosphate induces actin-based movement of raft-enriched vesicles through WASP-Arp2/3. Curr Biol 2000;10:311–320. [PubMed: 10744973]

Samarin S, Romero S, Kocks C, Didry D, Pantaloni D, Carlier MF. How VASP enhances actin-based motility. J Cell Biol 2003;163:131–142. [PubMed: 14557252]

Snapper SB, Takeshima F, Anton I, Liu CH, Thomas SM, Nguyen D, Dudley D, Fraser H, Purich D, Lopez-Ilasaca M, et al. N-WASP deficiency reveals distinct pathways for cell surface projections and microbial actin-based motility. Nat Cell Biol 2001;3:897–904. [PubMed: 11584271]

Soo FS, Theriot JA. Adhesion controls bacterial actin polymerization-based movement. Proc Natl Acad Sci U S A 2005;102:16233–16238. [PubMed: 16251274]

Spinardi L, Rietdorf J, Nitsch L, Bono M, Tacchetti C, Way M, Marchisio PC. A dynamic podosome-like structure of epithelial cells. Exp Cell Res 2004;295:360–374. [PubMed: 15093736]

Taunton J, Rowning BA, Coughlin ML, Wu M, Moon RT, Mitchison TJ, Larabell CA. Actin-dependent propulsion of endosomes and lysosomes by recruitment of N-WASP. J Cell Biol 2000;148:519–530. [PubMed: 10662777]

Upadhyaya A, Chabot JR, Andreeva A, Samadani A, van Oudenaarden A. Probing polymerization forces by using actin-propelled lipid vesicles. Proc Natl Acad Sci U S A 2003;100:4521–4526. [PubMed: 12657740]

Uruno T, Liu J, Li Y, Smith N, Zhan X. Sequential interaction of actin-related proteins 2 and 3 (Arp2/3) complex with neural Wiscott-Aldrich syndrome protein (N-WASP) and cortactin during branched actin filament network formation. J Biol Chem 2003;278:26086–26093. [PubMed: 12732638]

van der Gucht J, Paluch E, Plastino J, Sykes C. Stress release drives symmetry breaking for actin-based movement. Proc Natl Acad Sci U S A 2005;102:7847–7852. [PubMed: 15911773]

Vavylonis D, Kovar DR, O'Shaughnessy B, Pollard TD. Model of formin-associated actin filament elongation. Mol Cell 2006;21:455–466. [PubMed: 16483928]

Welch MD, Mullins RD. Cellular control of actin nucleation. Annu Rev Cell Dev Biol 2002;18:247–288. [PubMed: 12142287]

Wiesner S, Helfer E, Didry D, Ducouret G, Lafuma F, Carlier MF, Pantaloni D. A biomimetic motility assay provides insight into the mechanism of actin-based motility. J Cell Biol 2003;160:387–398. [PubMed: 12551957]

Yamaguchi H, Miki H, Suetsugu S, Ma L, Kirschner MW, Takenawa T. Two tandem verprolin homology domains are necessary for a strong activation of Arp2/3 complex-induced actin polymerization and induction of microspike formation by N-WASP. Proc Natl Acad Sci U S A 2000;97:12631–12636. [PubMed: 11058146]

Yarar D, To W, Abo A, Welch MD. The Wiskott-Aldrich syndrome protein directs actin-based motility by stimulating actin nucleation with the Arp2/3 complex. Curr Biol 1999;9:555–558. [PubMed: 10339430]

Yarar D, Waterman-Storer CM, Schmid SL. A dynamic actin cytoskeleton functions at multiple stages of clathrin-mediated endocytosis. Mol Biol Cell 2005;16:964–975. [PubMed: 15601897]

Zamanian JL, Kelly RB. Intersectin 1L guanine nucleotide exchange activity is regulated by adjacent src homology 3 domains that are also involved in endocytosis. Mol Biol Cell 2003;14:1624–1637. [PubMed: 12686614]

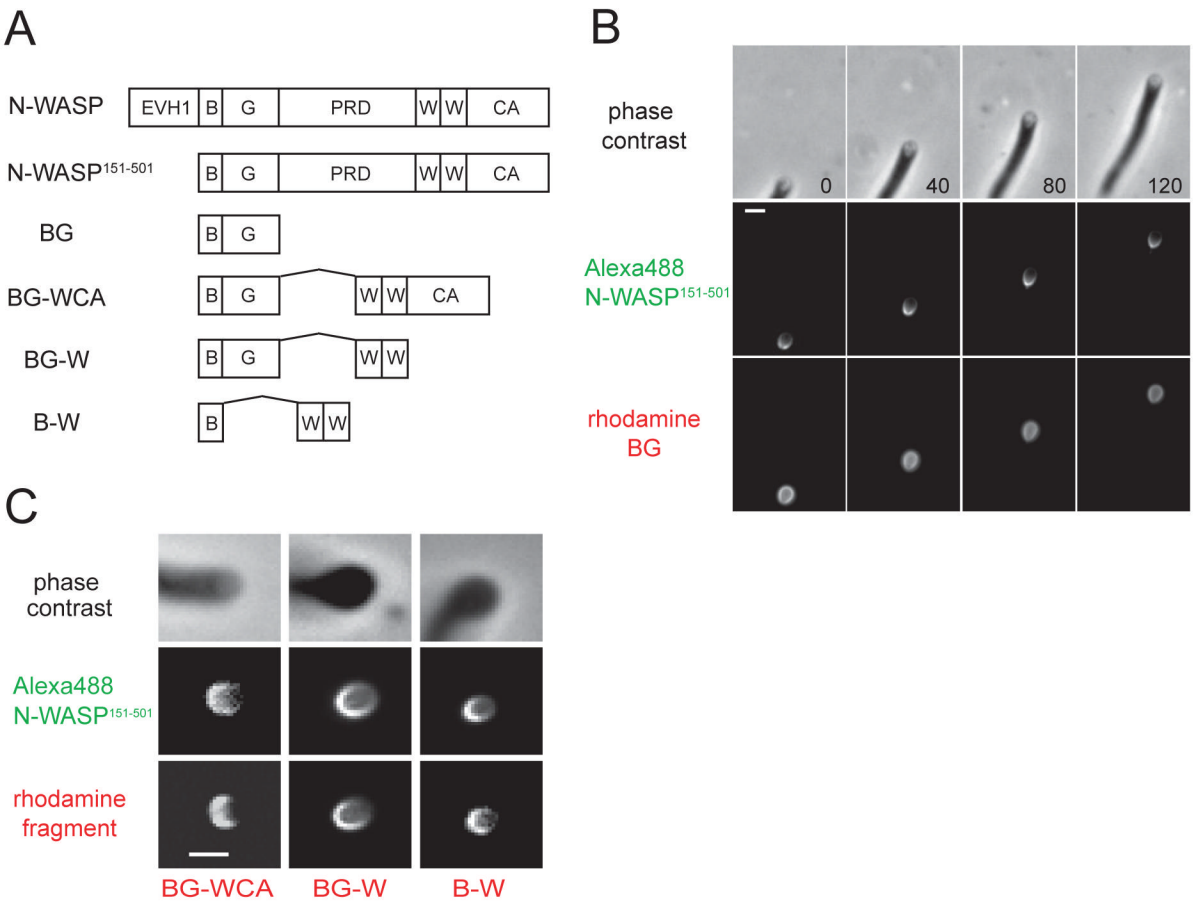

Fig 1. N-WASP WH2 domains localize to the attachment zone of moving vesicles

(A) Domain structure of N-WASP and derived fragments. Abbreviations: EVH1, Enabled-VASP homology domain 1; B, polybasic region; G, GTPase-binding domain; PRD, proline-rich domain; W, WASP homology domain 2; CA, central and acidic domain. Internally deleted domains were replaced with a $(Gly\text{-}Ser)_4$ linker.

(B) Alexa488 N-WASP$^{151\text{-}501}$ and rhodamine BG (each at 50 nM) were added to phorbol ester-stimulated Xenopus egg extracts, and rocketing vesicles were imaged every 40 s by phase contrast and fluorescence microscopy.

(C) Alexa488 N-WASP$^{151\text{-}501}$ and the indicated rhodamine-labeled fragments (final concentration, 50 nM) were imaged as in (B). Images are representative of >50 rocketing vesicles for each rhodamine-labeled fragment. Bar=2 μm.

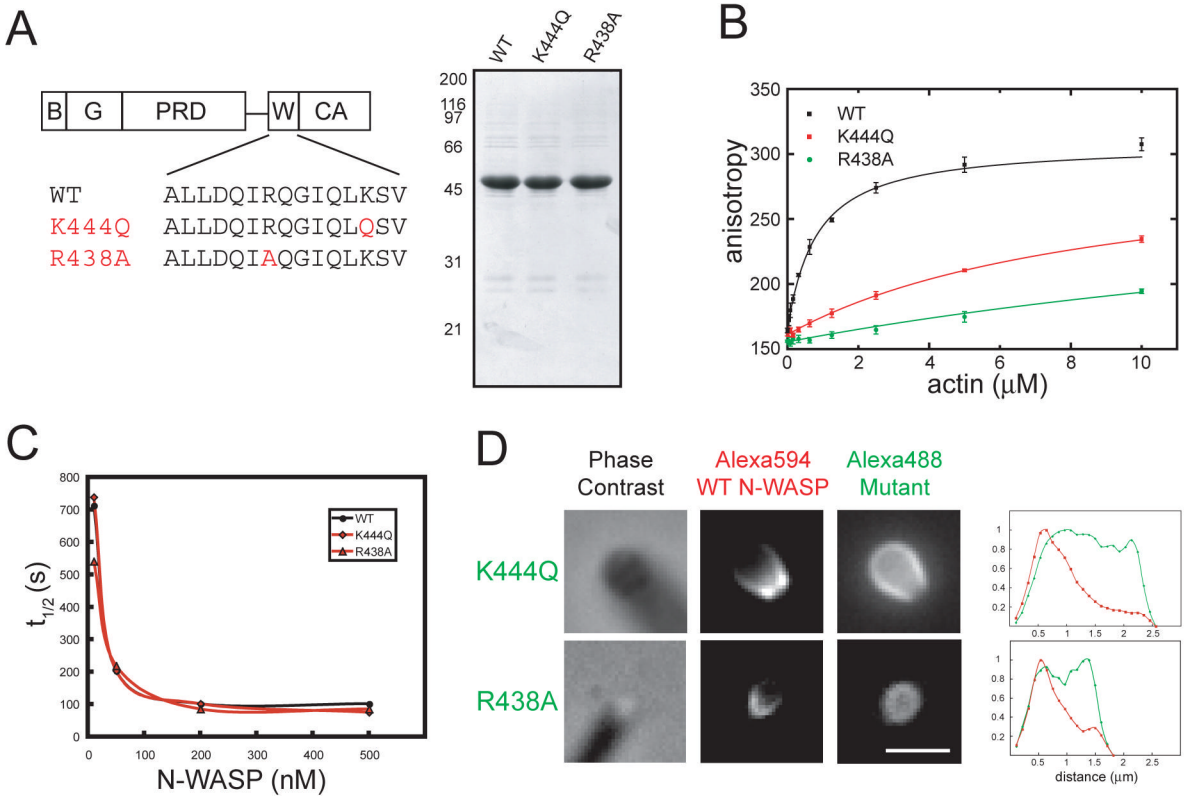

Fig 2. WH2 mutations uncouple nucleation promoting and asymmetric localization functions

(A) $WH2_b$ domain of $\delta WH2_a$ N-WASP$^{151\text{-}501}$ ("WT N-WASP"), highlighting K444Q and R438A mutations. SDS-PAGE of purified N-WASP proteins stained with Coomassie blue.

(B) Fluorescence anisotropy of Oregon Green N-WASP (100 nM of WT, K444Q, and R438A WCA fragments) in the presence of increasing concentrations of actin monomers (mean±S.D., n=4).

(C) Pyrene actin polymerization stimulated by N-WASP in the presence of saturating Cdc42/GTPγS (6 μM), 2.5 μM actin monomers (5% pyrene labeled), and 20 nM Arp2/3 complex. Plots indicate the time to half-maximal polymerization ($t_{1/2}$) as a function of N-WASP concentration. Raw data are shown in Fig. S1.

(D) Alexa594 WT N-WASP and either Alexa488 K444Q or R438A N-WASP (final concentrations, 50 nM) were added to phorbol ester-stimulated Xenopus egg extracts and rocketing vesicles imaged as in Fig. 1. Line-scan analysis (normalized fluorescence) indicates asymmetric localization of WT N-WASP (red lines), whereas K444Q and R438A N-WASP (green lines) are symmetrically localized or partially excluded from the attachment zone (representative of >50 rocketing vesicles). Bar=2 μm.

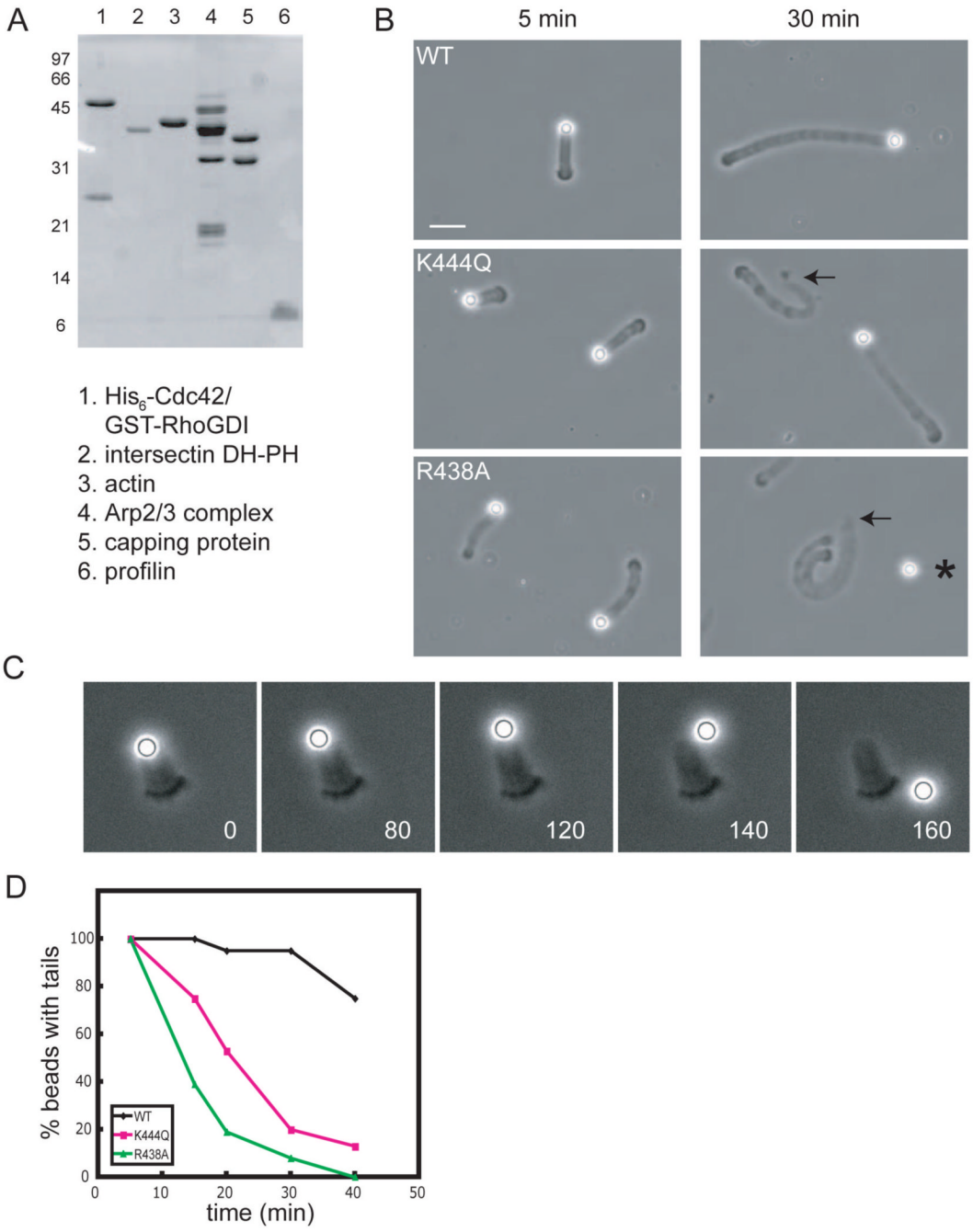

Fig 3. Reconstitution of membrane movement from pure components: WH2 mutations induce catastrophic detachment of actin comet tails

(A) SDS-PAGE of purified proteins (stained with Coomassie blue) used to reconstitute motility of lipid bilayer-coated glass beads.

(B) Phase-contrast images of motility reactions acquired 5 and 30 min after initiation. Arrows indicate detached actin comet tails; asterisk indicates a detached lipid-coated bead. Bar=10 μm.

(C) Time-lapse sequence showing catastrophic detachment of a lipid-coated bead from its comet tail (R438A N-WASP).

(D) Time course of comet tail detachment. At the indicated time points, motility reactions were fixed with 1.5% glutaraldehyde and the percentage of beads with attached tails was determined (40 beads per time point).

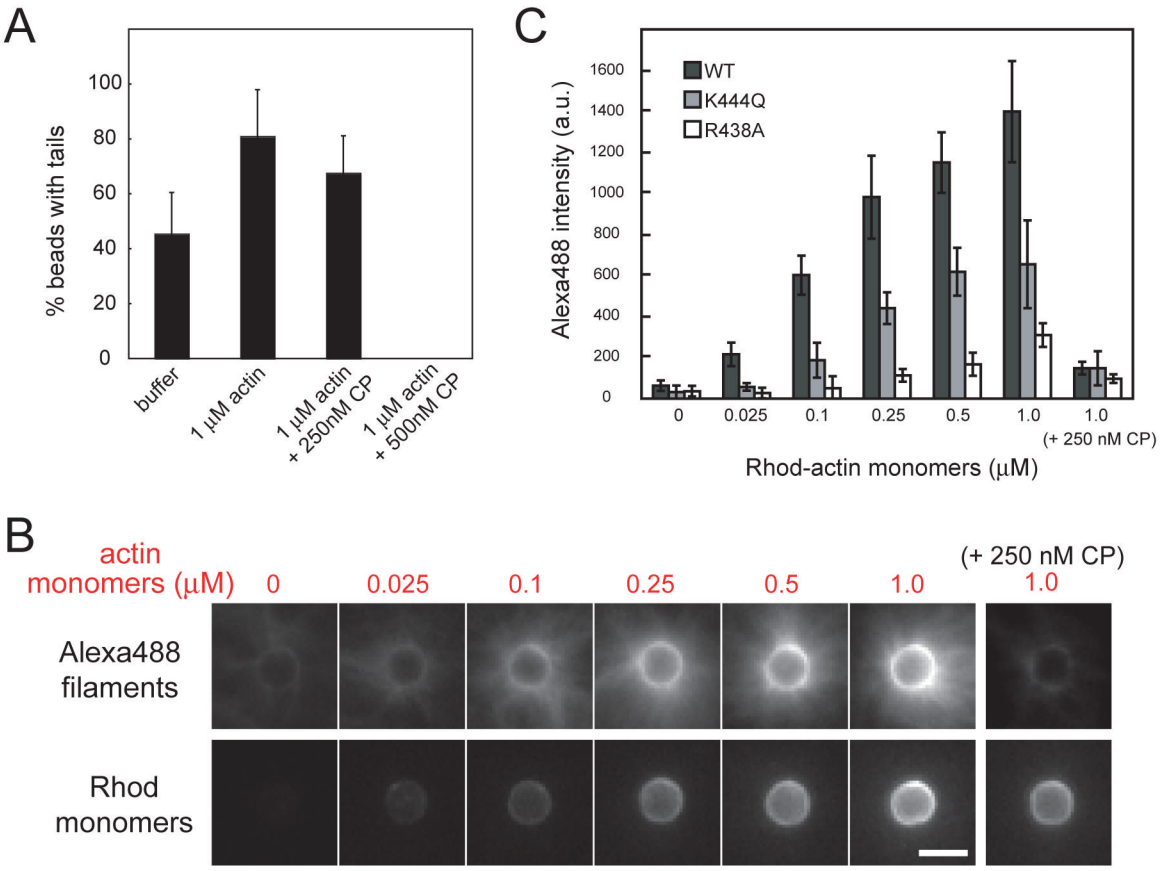

Fig 4. Comet tail attachment requires interactions between WH2 domains and actin filament barbed ends

(A) Motility reactions containing WT N-WASP were diluted 4-fold (at t=10 min) into buffer alone or buffer containing 1 μM actin plus the indicated concentrations of capping protein (CP). After 15 min, reactions were fixed in 1.5% glutaraldehyde and the percentage of beads with attached tails was determined (40 beads counted for each condition; shown are mean±S.D. percentages from 4 independent experiments).

(B) Polystyrene beads were coated with N-WASP (WT, K444Q, and R438A) and incubated with Alexa488 phalloidin-stabilized actin filaments (±capping protein) and increasing concentrations of latrunculin-stabilized actin monomers (17% rhod-labeled). Shown are images of WT N-WASP beads with bound Alexa488 filaments (upper panels) and rhod-actin monomers (lower panels).

(C) Fluorescence intensity of Alexa488 filaments bound to WT and mutant N-WASP beads (mean±S.D., n=15-20 beads for each condition). Bar=2 μm.

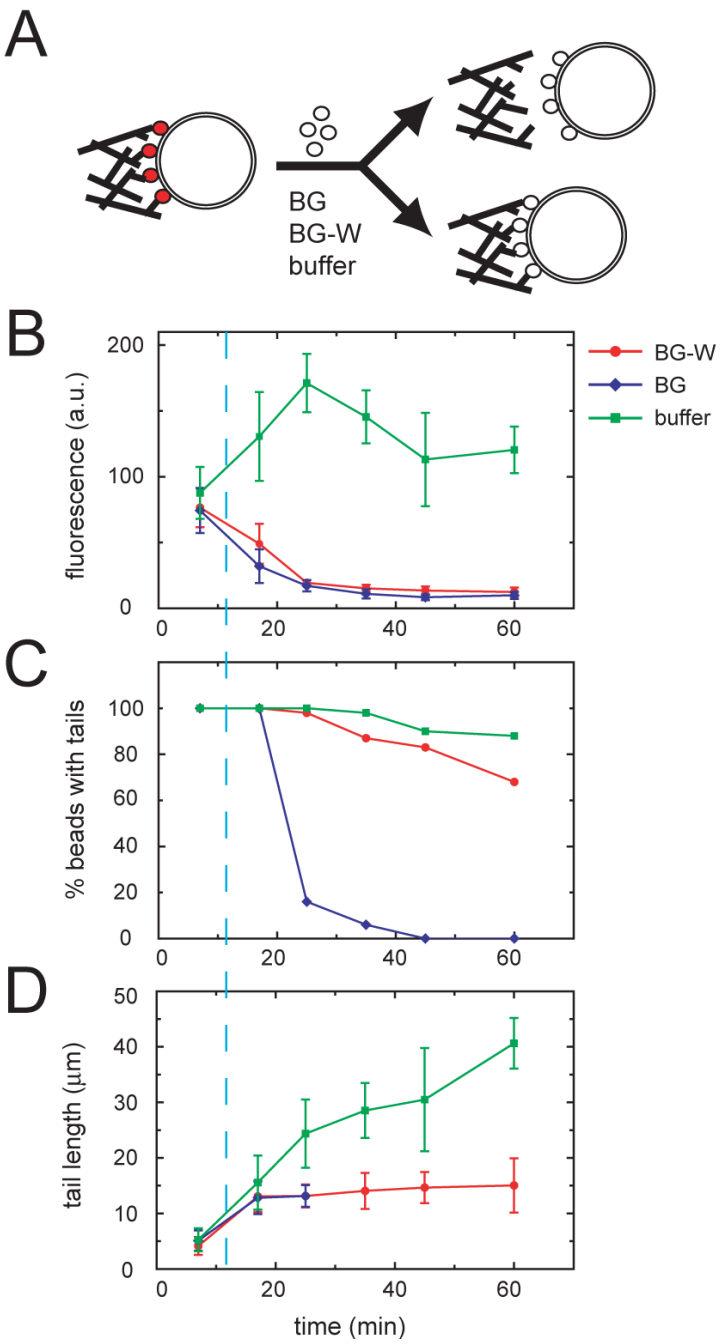

Fig 5. Barbed end capture by WH2 domains is sufficient to maintain actin network attachment

(A) N-WASP replacement experiment. Actin comet tails were assembled in standard motility reactions containing 150 nM Alexa488 N-WASP. At t=12 min, N-WASP fragments (BG or BG-W, 2 μM) or buffer was added to displace Alexa488 N-WASP from the lipid-coated beads. At the indicated time points, aliquots were fixed and analyzed as shown in the graphs.

(B) Bead-associated Alexa488 N-WASP fluorescence (mean±S.D., n=10 beads per time point).

(C) Percentage of beads with attached tails (n=40 beads per time point).

(D) Actin comet tail lengths (mean±S.D., n=10-15 tails per time point).

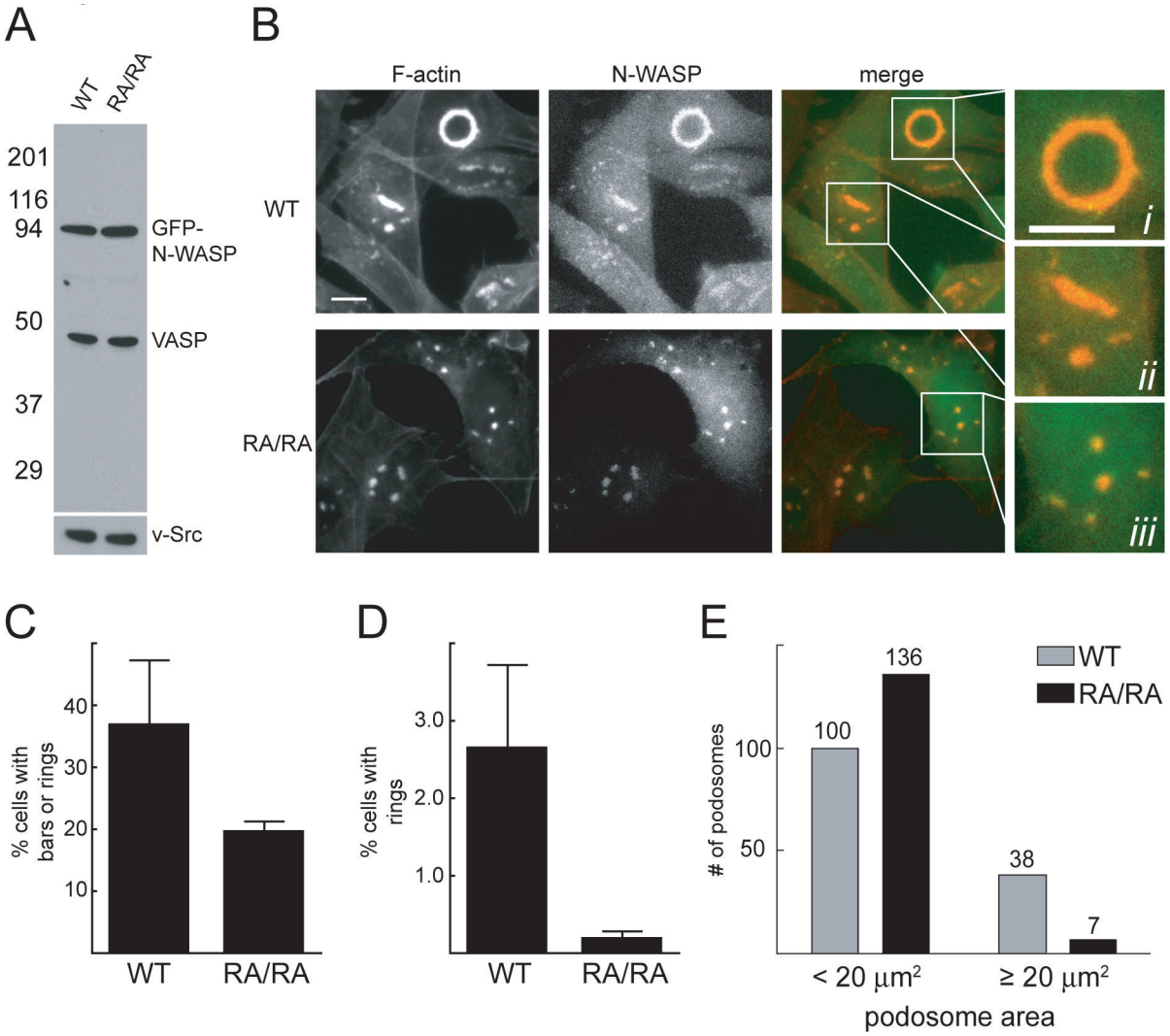

Fig 6. WH2 mutations disrupt podosome assembly in v-Src-transformed cells

(A) Western blot of v-Src-transformed N-WASP$^{-/-}$ fibroblasts rescued by retroviruses encoding full-length WT or R410A/R438A (RA/RA) GFP-N-WASP. WT and RA/RA cells show similar expression levels of GFP-N-WASP, v-Src, and VASP.

(B) Representative images of WT and RA/RA GFP-N-WASP cells 24 h after plating on fibronectin-coated coverslips. Cells were fixed, stained with Alexa594-phalloidin, and visualized by fluorescence microscopy. Boxed regions are magnified to display three podosome classes: (i) rings, (ii) bars, and (iii) puncta. Bar=10 μm.

(C) Percentage of podosome-positive cells with bars or rings (mean±S.D. from 3 independent experiments, $p<0.03$).

(D) Percentage of podosome-positive cells with rings (mean±S.D. from 3 independent experiments, $p<0.01$).

(E) Areas of podosome rings, bars, and puncta were measured in 50 randomly selected WT and RA/RA cells, all of which contained at least one podosome bar or ring. Areas were binned as shown (for reference, the ring in Fig. 6B has an area of 64 μm^2, whereas the bar has an area of 20 μm^2).

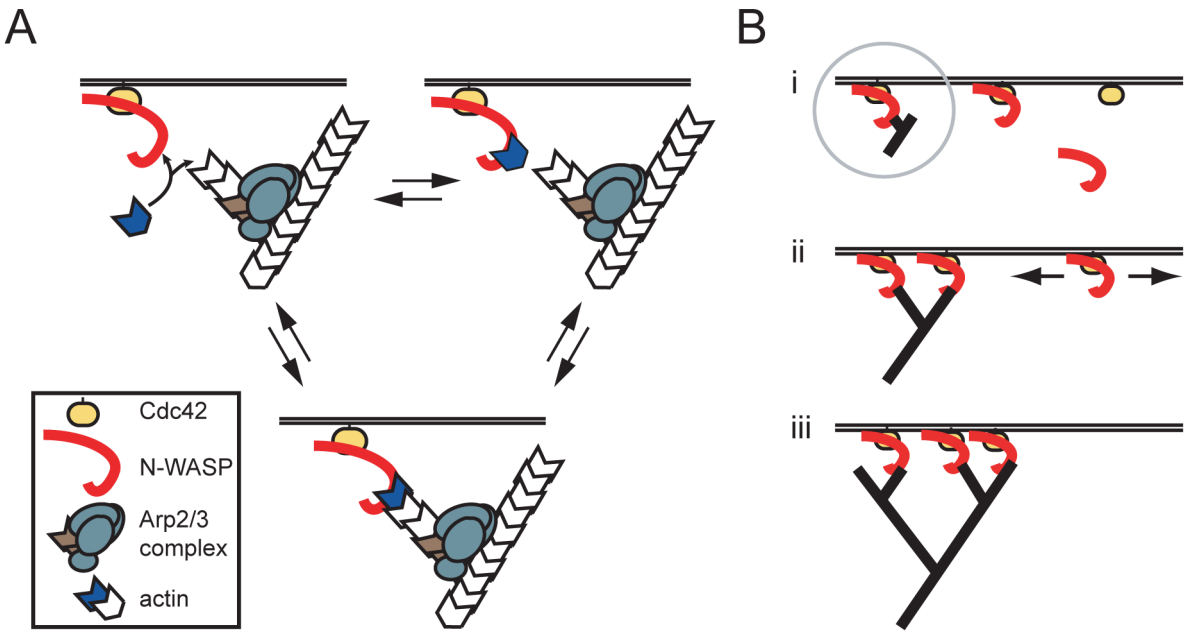

Fig 7. Dual role of WH2/barbed end interactions: membrane attachment and signal amplification

(A) Membrane-proximal barbed ends encounter a high local concentration of N-WASP/Cdc42 and enter a cycle of elongation, attachment, and release. Attachment of the dendritic network occurs when a critical number of filament barbed ends interact with WH2 domains. Upon dissociation of the attachment complex, rapid rebinding can occur because of the high density of barbed ends and N-WASP and the inability of actin filaments in the dendritic network to rapidly diffuse away.

(B) Nascent barbed ends created by dendritic nucleation (i) can capture N-WASP/Cdc42 complexes that diffuse within the plane of the membrane (ii). Subsequent nucleation and branch formation locally increases the number of barbed ends, which in turn concentrates more N-WASP molecules (iii).